J Neurophysiol
88: 2422–2429, 2002; 10.1152/jn.00598.2002.

Frequency Selectivity of Layer II Stellate Cells in the Medial Entorhinal Cortex

JULIE S. HAAS AND JOHN A. WHITE
Department of Biomedical Engineering, Center for BioDynamics, Boston University, Boston, Massachusetts 02215

Received 18 March 2002; accepted in final form 24 July 2002

Haas, Julie S. and John A. White. Frequency selectivity of layer II stellate cells in the medial entorhinal cortex. *J Neurophysiol* 88: 2422–2429, 2002; 10.1152/jn.00598.2002. Electrophysiologically, stellate cells (SCs) from layer II of the medial entorhinal cortex (MEC) are distinguished by intrinsic 4- to 12-Hz subthreshold oscillations. These oscillations are thought to impose a pattern of slow periodic firing that may contribute to the parahippocampal theta rhythm in vivo. Using stimuli with systematically differing frequency content, we examined supra- and subthreshold responses in SCs with the goal of understanding how their distinctive characteristics shape these responses. In reaction to repeated presentations of identical, pseudo-random stimuli, the reliability (repeatability) of the spiking response in SCs depends critically on the frequency content of the stimulus. Reliability is optimal for stimuli with a greater proportion of power in the 4- to 12-Hz range. The simplest mechanistic explanation of these results is that rhythmogenic subthreshold membrane mechanisms resonate with inputs containing significant power in the 4- to 12-Hz band, leading to larger subthreshold excursions and thus enhanced reliability. However, close examination of responses rules out this explanation: SCs do show clear subthreshold resonance (i.e., selective amplification of inputs with particular frequency content) in response to sinusoidal stimuli, while simultaneously showing a lack of subthreshold resonance in response to the pseudo-random stimuli used in reliability experiments. Our results support a model with distinctive input-output relationships under subthreshold and suprathreshold conditions. For suprathreshold stimuli, SC spiking seems to best reflect the amount of input power in the theta (4–12 Hz) frequency band. For subthreshold stimuli, we hypothesize that the magnitude of subthreshold theta-range oscillations in SCs reflects the total power, across all frequencies, of the input.

INTRODUCTION

The medial entorhinal cortex (MEC) serves as an information gateway between the neocortex and hippocampus and thus plays a major role in any conceptual or computational model of hippocampal function (Witter et al. 1989). Entorhinal output to the hippocampus comes from the superficial layers, especially layer II, in which the majority of principal cells are spiny stellate cells (SCs).

The electrophysiological properties of layer II SCs are distinctive. In vitro, SCs generate 4- to 12-Hz subthreshold oscillations in membrane potential in response to small, constant-current stimuli (Alonso and Klink 1993; Alonso and Llinás 1989). With increasing input magnitude, occasional action potentials arise, phase-locked to the underlying subthreshold oscillations. Because the subthreshold oscillations constrain firing to 4–12 spikes/s (for intermediate stimulus magnitudes) in SCs, those oscillations have been hypothesized to contribute to the theta rhythm, an electroencephalographic (EEG) rhythm of similar frequency range seen commonly throughout the hippocampal region under conditions like active exploration (Alonso and Klink 1993; Bland and Colom 1993; Hasselmo et al. 2000). Similar oscillatory behavior is seen in many neural populations, suggesting a general mechanism of synchronization of coupled neuronal "resonators" (see review by Hutcheon and Yarom 2000). In addition to potentially promoting synchrony, the intrinsically rhythmic electrophysiological properties of SCs and other neurons seem certain to filter and transform the temporal properties of their inputs in interesting, largely unexplored ways.

The mechanisms underlying subthreshold oscillations and phase-locked firing in SCs are reasonably well understood. Subthreshold oscillations are generated by interactions between a persistent Na^+ current and a slow opposing current, which may include contributions from the slow, hyperpolarization-activated cation current I_h, and a slowly activating K^+ current (Dickson et al. 2000; Eder et al. 1991; Hasselmo et al. 2000; Klink and Alonso 1993; White et al. 1995). The number of Na^+ channels underlying the persistent Na^+ current is less than 5,000, small enough that "channel noise" from the gating of these Na^+ channels contributes significantly to the cells' electrophysiological properties in computational studies (White et al. 1998, 2000).

As SCs temporally transform their inputs, some general aspect of their responses must be reliable (repeatable) for the information contained within the input to be later retained or recalled. Our goal in the present work is to understand more clearly how robustly and reliably MEC SCs respond to inputs with various temporal structures. Based on past work, we might expect three results. First, in response to repeated presentations of a given stimulus, the high degree of intrinsic channel noise present in SCs (White et al. 1998) may render their responses unreliable compared with those that have been reported in other preparations (Mainen and Sejnowski 1995). Indeed, the present results indicate this possibility, although it is difficult to make such comparisons using data collected in different cellular populations using different recording and data analysis techniques. Second, because firing rates in SCs are biophysically constrained to the range 4–12 spikes/s for inter-

Address reprint requests to: J. A. White (E-mail: jwhite@bu.edu).

The costs of publication of this article were defrayed in part by the payment of page charges. The article must therefore be hereby marked "*advertisement*" in accordance with 18 U.S.C. Section 1734 solely to indicate this fact.

mediate stimulus magnitudes (Alonso and Llinás 1989), we might expect that SCs respond preferentially reliably to inputs with more power in this range of frequencies, in analogy with past results from mathematical models (Jensen 1998) and other experimental preparations (Fellous et al. 2001; Hunter et al. 1998). Again, the present results largely match expectations in this regard. Third, because neuronal subthreshold oscillations are often described using the analogy of linear circuits with electrical resonance (see review by Hutcheon and Yarom 2000), we might expect a priori that subthreshold behavior in SCs would approximate the behavior of a linear resonator. Further, we might hypothesize that a model including linear resonance in the subthreshold regime, with a fixed voltage threshold for spiking, would serve to explain the frequency dependence of reliability. In this case, the present results do not match expectations. We see an absence of frequency preference in response to complex stimuli, along with strong evidence of nonlinearity in the subthreshold regime. The observed enhancement in reliability, without an accompanying subthreshold resonance, suggests that traditional means of studying neuronal resonance may lead to misleading expectations or results in some cases. Our results point to a more complex source of reliability in SCs, in which SCs show distinctively different input-output relationships in the sub- and suprathreshold regimes. Some of this work has previously appeared in preliminary form (Haas and White 1999, 2000).

METHODS

All experiments were conducted as approved by the Boston University Institutional Animal Care and Use Committee. Young (14- to 35-days old) Long-Evans rats were anesthetized by overexposure to CO_2 and decapitated. The brain was quickly removed and immersed in cold (0°C) oxygenated artificial cerebrospinal fluid (ACSF) (in mm: 126 NaCl 3 KCl, 1.25 NaH_2Po_4, 2 $MgSO_4$, 26 $NaHCO_3$, 10 glucose, and 2 $CaCl_2$, buffered to pH 7.4 with 95/5% O_2-CO_2). Horizontal slices were prepared using a Vibratome cutter (TPI). Slices were allowed to recover for 1 h prior to recording in a holding chamber at room temperature, continuously bathed in oxygenated artificial cerebrospinal fluid (ACSF). The recording chamber was a Haas top (Harvard Apparatus), maintained at 34°C (TC202-A, Harvard Apparatus). Layer II of the EC was visualized by transillumination of the recording chamber. Electrodes of resistance 70–90 MΩ were pulled on a horizontal puller (Sutter Instruments) and filled with 2 M KCl. Intracellular voltages were amplified (Axoclamp 2B, Axon Instruments), low-pass filtered (lab-made 8-pole Butterworth at 5 kHz), and digitized at 10 kHz via software created in LabView (National Instruments) controlling a dedicated-processor I/O board (DAP3200a, Microstar Laboratories). In most experiments, synaptic transmission was blocked by 6-cyano-7-nitroquinoxalene-2,3-dione (CNQX, 10 μM), bicuculline methiodide (10 μM), and D-2-amino-5-phosphonopentanoic acid (AP-5, 30 μM), obtained from Sigma (St. Louis, MO). Even without synaptic blockers, spontaneous synaptic events were too rare and too small to change any of our results.

We selected SCs by the unique characteristics of their electrophysiological responses to long current steps: a prominent (more than 30%) sag in response to both depolarizing and hyperpolarizing currents, as well as an early first spike (e.g., Fig. 1*A*) in response to suprathreshold stimuli (Alonso and Klink 1993). Fluctuating stimuli presented to SCs had two components. The first component was an underlying DC current, chosen to keep the cell just at or below threshold (defined operationally as a DC stimulus for which the cell fired twice or less during a 500-ms stimulus presentation). The second stimulus component was a zero-meaned fluctuating signal, composed of a Gaussian white noise signal (newly generated for each trial)

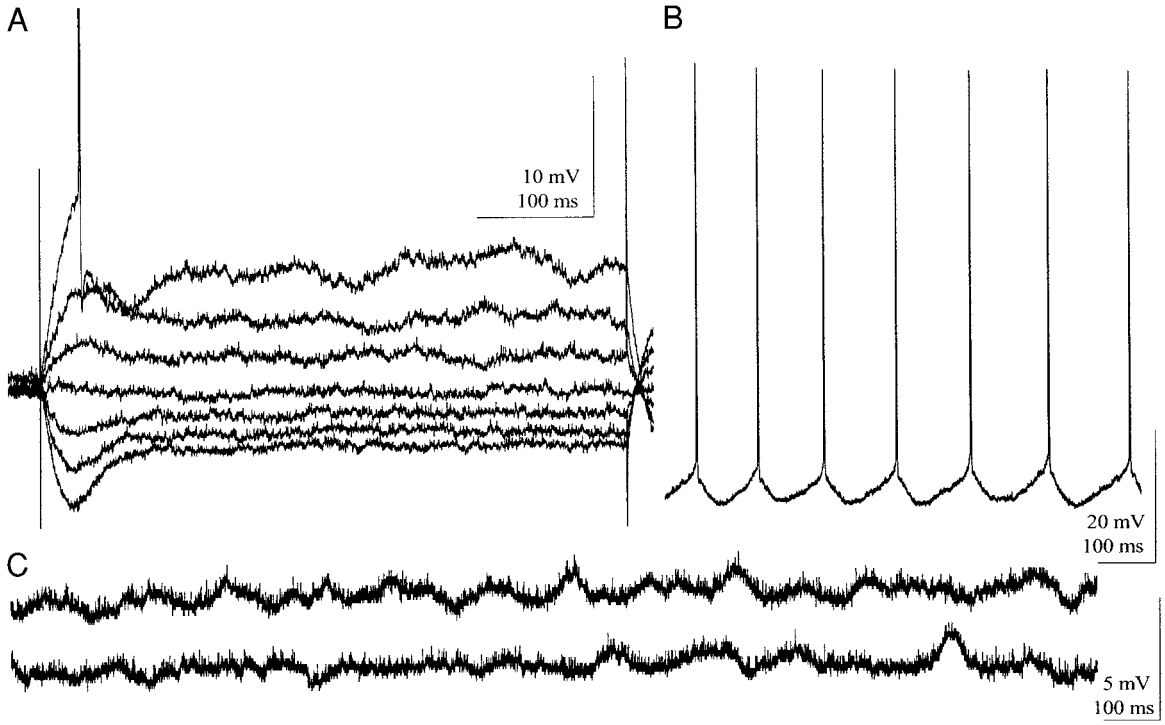

FIG. 1. Response of stellate cells (SCs) to DC current injection. Several characteristic electrophysiological features are evident, including a sizable inward "sag" in voltage after the onset of a current pulse (*A;* injected currents from −300 to +300 pA in steps of 100 pA), theta-frequency spiking (*B;* injected current of 400 pA), and subthreshold activity with clear theta-frequency content (*C;* injected current of 50 pA).

convolved with a low-pass filter [impulse response $h(t) = e^{-t/\tau}$, $t \geq 0$; cutoff frequency $= 1/2\pi\tau$].

To assess the specific effects of theta-range frequency content on SCs, we used three values of the low-pass time constant τ. In the first case, we set $\tau = 3$ ms, corresponding to a low-pass cutoff frequency of 53 Hz. These stimuli, which we refer to as *broadband*, had a distribution of {3.5, 10.3, 86.2} percent of total power in the {0–3.9, 4–11.9, 12–5,000} Hz frequency bands. [Calculations of power were made using fast Fourier transform (FFT)-based techniques on the body of signals used in experiments. FFT-based results match theoretical values closely.]. The second stimulus type, which we refer to as *theta-rich*, had a time constant $\tau = 20$ ms, corresponding to a low-pass cutoff of 8 Hz and a distribution of {20.6, 37.7, 41.7} percent power in the {0–3.9, 4–11.9, 12–5,000} Hz frequency bands. The third stimulus type, which we refer to as *sub-theta*, had a time constant $\tau = 80$ ms, so that the low-pass cutoff of 2 Hz was just below the range of theta frequencies. Sub-theta stimuli had significant power in the theta range but were dominated by the lowest frequencies, with percent powers of {52.8, 31.5, 15.7} in the {0–3.9, 4–11.9, 12–5,000} Hz bands. Use of the sub-theta stimulus allowed us to test the null hypothesis that any differences in responses to broadband and theta-rich stimuli were due to the presence of low-frequency power rather than power specifically in the theta band. A normalization procedure yielded stimuli that were matched in overall amounts of current fluctuation [σ_i, the root-mean-square (RMS) magnitude of the fluctuation] but with different distributions of power over each frequency band, as quantified in the preceding text. Each "frozen noise" input was delivered 10 times per trial, with a long (1–2 s) rest between repetitions. Trials were randomized over values of σ_i.

Off-line analysis was performed using Matlab (Mathworks, Natick, MA) and Origin (OriginLab, Northhampton, MA) software. We calculated reliability as the average normalized cross-correlation, within a 2-ms window of delay, of the 10-point processes (each convolved with a decaying single exponential with an interaction time constant $\tau_{int} = 3$ ms), representing the spike trains from each repeated presentation of the stimulus.

"Predicted" subthreshold responses of SCs (Fig. 5, *C* and *D*) were generated using the methods of linear systems theory, which dictates that any linear system simply filters its inputs in an input-independent manner. We derived the filtering function, also known as the frequency response function, by measuring responses to sinusoidal inputs over a range of frequencies (e.g., Fig. 4*A*). A fifth-order polynomial was fit to these responses to generate a smooth estimate of frequency response in SCs. A normalized version of this estimated frequency response curve was then used to predict the amount by which input bandwidth should differentially affect total RMS output (Fig. 5*C*). We normalized the frequency response curve by the average SC input resistance (40 MΩ) to produce the predicted output frequency spectra (Fig. 5*D*) in response to inputs of differing bandwidth but identical total power.

Statistical analysis was performed using the Matlab function ANOVAN, which allowed us to calculate two-factor ANOVA with repeated measures. This test allowed us to assess the significance of effects of two factors (e.g., input bandwidth and the RMS value of the input) simultaneously, as well as estimating the probability of interaction between the two factors. Results are reported as insignificant for cases in which $P > 0.05$.

RESULTS

Basic response properties

Figure 1 shows typical recorded responses of SCs to intracellularly applied DC stimuli. Several previously documented, identifying response properties (Alonso and Klink 1993) of these cells are evident, including a prominent "sag" in response to hyperpolarizations (Fig. 1*A*), the early first appearance of a spike (Fig. 1*A*), subthreshold oscillations of frequency 5–10 Hz (Fig. 1*C*), and theta-frequency spiking (Fig. 1*B*). These responses to relatively simple DC inputs reveal some of the intrinsic dynamics that shape cellular responses to more complex inputs.

Frequency-sensitive reliability

Figure 2 shows the responses of a representative SC to two types of fluctuating-current input that we presented. Each cell was injected ten times with the same "frozen noise" current input. For broadband inputs (flat in their power spectra for frequencies less than 50 Hz; Fig. 2*A*), SCs responded reliably (i.e., consistently from trial to trial) to the onset of a stimulus but less reliably afterward. In some cases, reliability was diminished by the "jitter" in spike arrival times (e.g., near $t =$ 200 ms in Fig. 2*A*). However, the more common cause of reduced reliability was that many stimulus features evoked output spikes with probability less than one (e.g., near $t = 400$ ms in Fig. 2*A*).

Spiking reliability is visibly higher in response to repeated presentations of theta-rich inputs (flat in their power spectra for frequencies less than 8 Hz; Fig. 2*B*) with the same level of RMS fluctuation σ_i. Each spike train, in the theta-rich input case, more closely resembles the other responses to that same noisy signal. Under these conditions, both spike-time precision and, especially, the probability of a spike in response to a given stimulus feature are enhanced.

Figure 2*C* shows summary reliability results for 27 SCs (mean resting potential, −70.6 mV; input resistance, 43.1 MΩ; and spike height, 73.9 mV), in which reliability (see METHODS) is plotted versus σ_i. The three curves correspond to the differences in the frequency content of the input. Consistent with the example in Fig. 2, *A* and *B*, reliability was enhanced for theta-rich inputs (solid line), as compared with responses to both broadband inputs (dashed line) and sub-theta inputs (inputs with power mostly at frequencies less than 4 Hz; dotted line). The effect is statistically significant, as determined by a two-way ANOVA with repeated measurements, comparing nonoverlapping theta-rich responses with broadband and sub-theta responses ($P < 0.05$ for the effect of input bandwidth on mean reliability, the effect of σ_i on reliability, and the interaction of effects of input bandwidth and σ_i in both comparisons).

Enhanced reliability with theta-rich stimulation is most notable by eye in the crucial range of input ($\tau_i < 50$ pA) for which overall reliability and firing rate are lower. Given our input resistances of 30–50 MΩ, in vivo measurements of fluctuations in membrane potential (Destexhe and Pare 1999) indicate that this range of input fluctuations is physiologically relevant. Results for $\sigma_i < 50$ pA are largely independent of the interaction time constant τ_{int} (which sets the temporal resolution of our analysis) because the dominant contributor to reliability for such inputs is the probability of spiking, rather than jitter in spike timing (data not shown). Specific values of the high-σ_i asymptotes of the curves do depend on τ_{int} (data not shown) because for high σ_i, cells fire with high probability, making jitter the dominant factor in limiting reliability. The relative positions of the asymptotes are independent of τ_{int}.

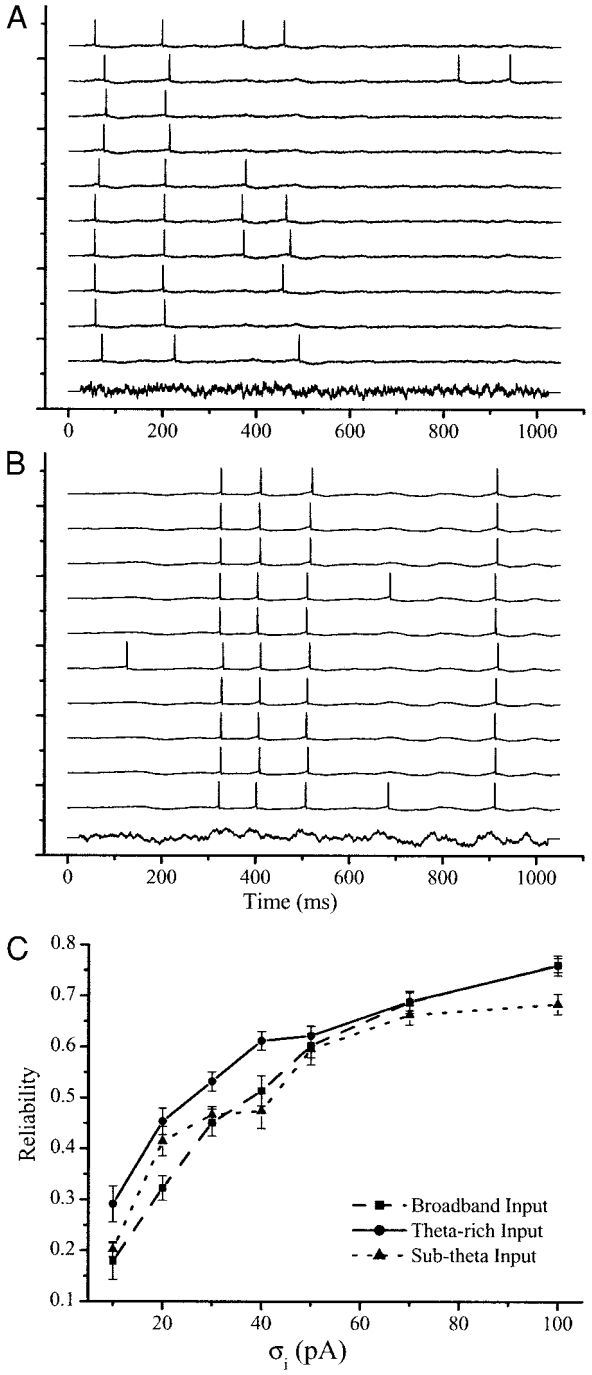

FIG. 2. Reliability depends on stimulus frequency content. *A* and *B*: responses of a single SC (resting potential = −63 mV, R_{in} = 53 MΩ) to 10 repetitions each of 2 types of fluctuating-current stimulus. Shown are 2 representative stimuli (*A* and *B, bottom;* 10 pA of DC underlying fluctuations with matched total RMS level σ_i = 40 pA, frequency content as described in METHODS) and 10 SC responses (*A* and *B,* 100 mV per vertical division) to the repeated presentations of those stimuli. *C*: plots of reliability vs. σ_i, the RMS level of fluctuating current input, demonstrate that SCs responded more reliably to input biased toward the theta range of frequencies (n = 27; mean ± SE).

Reverse correlations hint at a frequency preference

Using an input RMS value for which reliability was sensitive to bandwidth (τ_i = 40 pA), we plotted the reverse correlation function, which is the average current preceding a spike (Fig. 3*A*; we confined this analysis to reliable spikes, defined as spikes that occurred within a 10-ms window for at least 7 of 10 trials). We found that for all three bandwidths of input, current was integrated over a period of 25–40 ms to generate reliable spikes. This amount of time corresponds to a (rising) quarter-cycle of the theta rhythm and suggests that SCs select inputs that match their intrinsic dynamics when integrating for spiking. Temporally scaling the inputs by their respective time constants (Fig. 3*B*) reinforces this result. From the theta-rich

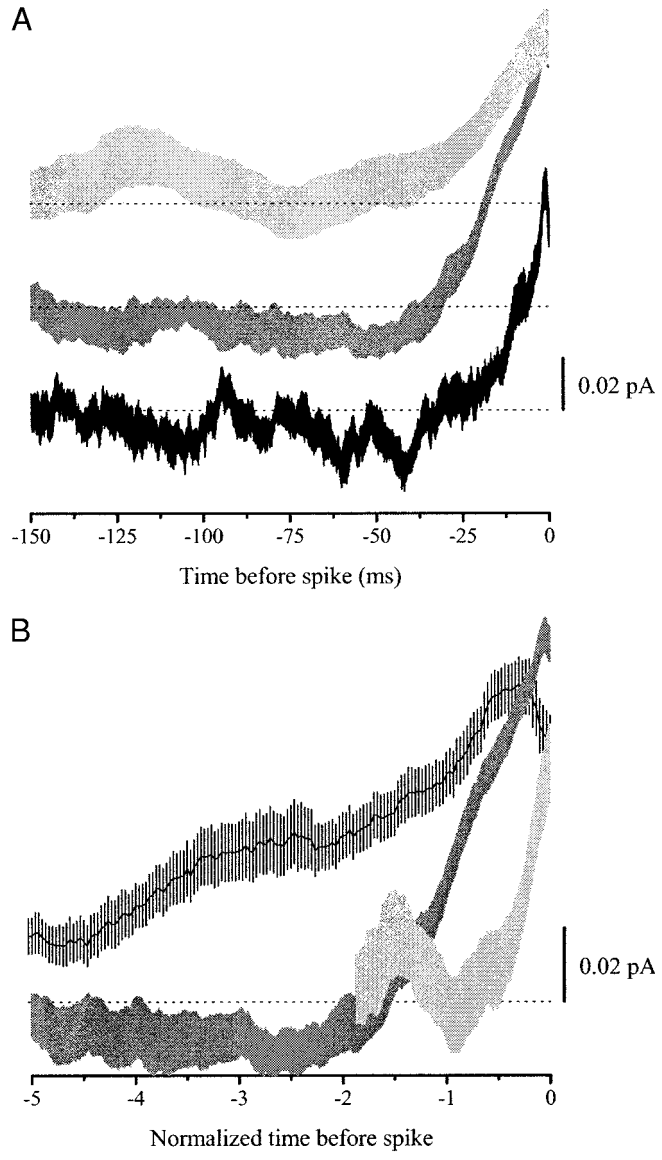

FIG. 3. Reverse correlations reveal temporal tuning in SCs. *A*: average fluctuations (mean ± SE) in current preceding a reliable spike (see text), for all 3 types of "frozen noise" input (black for broadband, dark gray for theta-rich, light gray for sub-theta). Horizontal dotted lines show the mean of the fluctuating component of the input preceding the spike (the DC offset, which differed between cells, was subtracted from each stimulus). Despite the differences in "natural" frequency content of the three stimuli, the rising phases of these three traces are remarkably similar. *B*: results from *A* re-plotted on a normalized time scale. Times were normalized by dividing by the time constant of the digital filter used to construct the stimuli (τ = 3 ms for broadband, 20 ms for theta-rich, 80 ms for sub-theta). For broadband stimuli (black), unusually slow (more than 5 τ) rising currents drove reliable spikes. For sub-theta stimuli (light gray), unusually fast (less than 0.5 τ) rising currents were required. For theta-rich stimuli (dark gray), the time course of the optimal rising current roughly matched the natural time scale of the stimulus (1–2 τ).

input (dark gray), SCs selected events roughly matching the time scale of that input (1 unit of the normalized time axis in Fig. 3*B*). From the faster broadband input (black), SCs selected unusually slow depolarizing events (over multiple time constants of that input). From slower sub-theta input (light gray), SCs selected unusually fast events (less than 1 normalized time unit) within that stimulus.

Resonance in response to pure and frequency-modulated sinusoidal stimuli

The most parsimonious explanation of frequency-dependent reliability in SCs is that 4- to 12-Hz subthreshold oscillations give rise to a resonant subthreshold response at these frequencies, with more reliable spiking associated with stimuli within the resonant range of frequencies simply because the subthreshold response to these stimuli is larger and thus more likely to cross threshold. From past work on the subject of oscillating and resonant neurons (see review by Hutcheon and Yarom 2000), we expect resonant behavior in SCs to be nearly *linear* in the subthreshold regime (i.e., to have input-output characteristics that do not depend on the nature of the stimulus for small-amplitude stimuli). To directly measure SCs' subthreshold resonance in a simple manner, we delivered small pure sinusoidal currents of varying frequencies to the SCs. Each sinusoid was added to an underlying DC pulse of amplitude equal to half the peak-to-peak amplitude of the sinusoid, so that the amplitude of the resulting sinusoidal input spanned a range from zero to full peak amplitude, and probed the majority of the subthreshold regime of the neuron. Amplitudes were chosen as the largest inputs failing to elicit a spike. Results (Fig. 4*A*) show a clear resonance in response to sinusoids in the theta range. Plots of the input-output phase difference (Fig. 4*B*) are somewhat flatter than one would expect for a classical resonant circuit, which would give phases approaching −180° for high-frequency stimuli, but limits in our ability to measure magnitudes and phases accurately for frequencies more than 20 Hz make this conclusion only tentative. Resonant responses were not seen for putative pyramidal cells, which were identified electrophysiologically by a significantly smaller sag (<15%) in voltage response to DC current injection (Alonso and Klink 1993).

Subthreshold resonance can be quantified more efficiently using frequency-modulated sinusoids, often referred to as "ZAP" stimuli (Gutfreund et al. 1995; Hutcheon and Yarom 2000; Hutcheon et al. 1996; Puil et al. 1986). Like responses driven by pure sinusoidal stimuli, normalized ZAP-driven responses (Fig. 4*C*) are very consistent among SCs and show clear evidence of subthreshold resonance in the theta range of frequencies. Responses to ZAP stimuli in putative pyramidal cells showed no signs of frequency resonance; their responses were maximal at the lowest frequency presented, and monotonically diminished thereafter (data not shown). Estimates of SC frequency responses driven by sinusoids and ZAPs differ in the minute details (data not shown), but not in the overall resonant electrophysiological profile.

Lack of resonance in response to frozen noise stimuli

SCs exhibit subthreshold resonance in response to pure sinusoidal or ZAP stimuli (Fig. 4). We also examined the

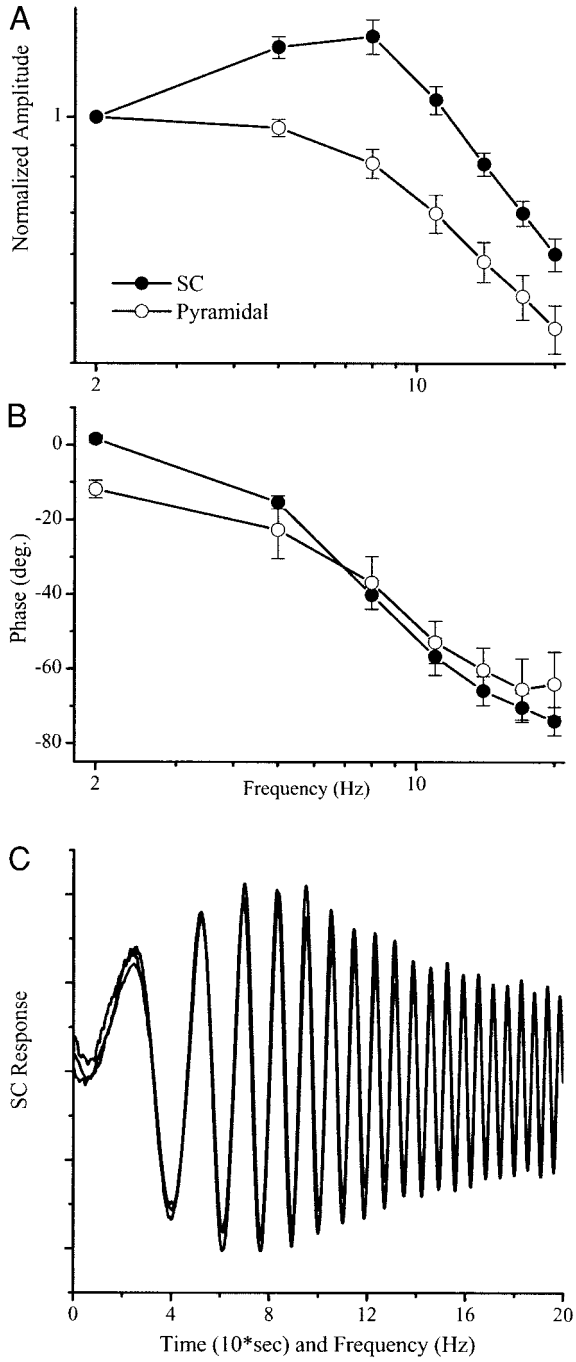

FIG. 4. Subthreshold responses to constant-frequency and frequency-modulated sinusoids show resonance. *A* and *B*: frequency response curves (magnitude and phase, mean ± SE). *C*: normalized subthreshold responses of SCs (responses from five cells, normalized by estimated input resistance) to a frequency-modulated sinusoidal ("ZAP") stimulus. These responses also show clear evidence of resonance in the theta band. Responses to ZAP stimuli do not indicate resonance in pyramidal cells (data not shown).

subthreshold portions of SC response to the frozen noise stimuli, looking for the hallmarks of resonance and linearity. For resonance, we focused on increased amplification of stimuli with more power within a particular frequency range. For linearity, we focused on a consistent input-output relationship for any stimulus.

In Fig. 5*A*, the experimentally measured root mean square (RMS) subthreshold voltage response (σ_v) is plotted versus the

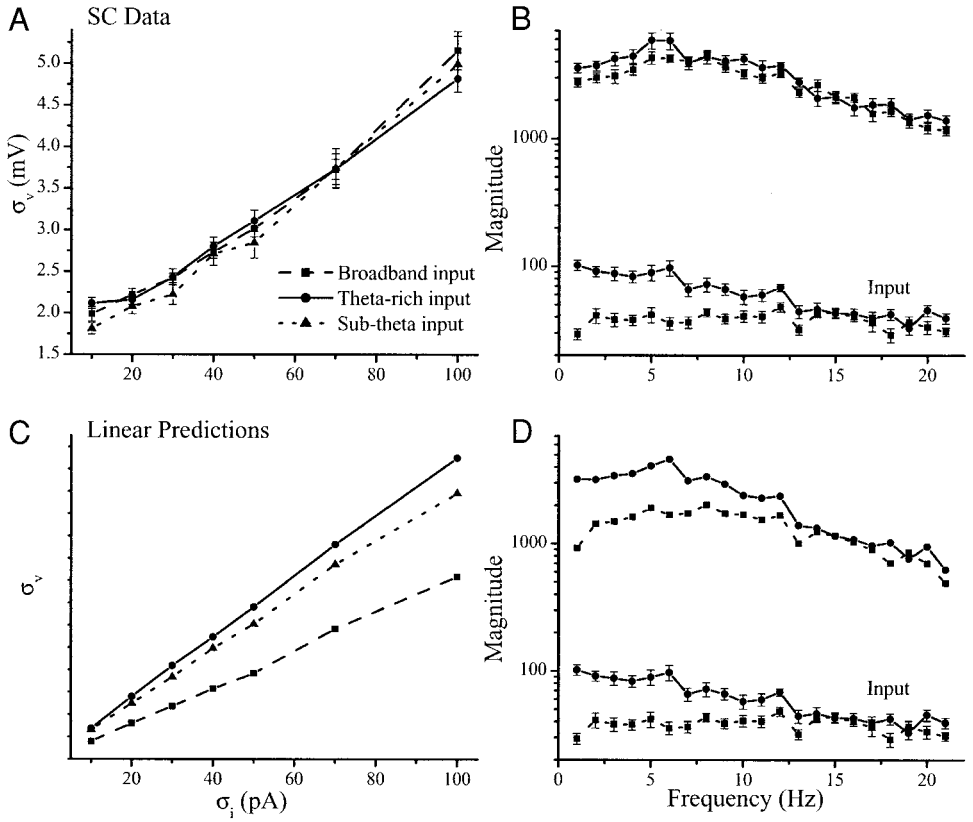

FIG. 5. Subthreshold responses to frozen noise stimuli are nonlinear and nonresonant. *A*: RMS value of SC output voltage response (σ_v, mV) plotted against input RMS current (σ_i, pA), for broadband, theta-rich, and sub-theta stimuli. *B*: averaged magnitudes of SC voltage responses (*top*; mV/$\sqrt{\text{Hz}}$), plotted versus frequency. *Bottom*: the spectra of the inputs (μA/$\sqrt{\text{Hz}}$). Results were derived by taking the FFT of the data, then calculating the magnitudes of the input and output at each value of frequency. For clarity, only broadband and theta-rich results are shown; sub-theta results are very similar. Remarkably, for inputs of significantly different frequency content, both the overall and frequency-distributed magnitude of the SC voltage responses were strikingly similar. *C*: predictions of subthreshold voltage responses to the 3 inputs (see METHODS for details). In the predicted responses, as opposed to their measured counterparts (*A*), resonance to sinusoidal inputs leads to larger slopes, or gain, for inputs with more frequency content within the resonant pass-band. These values are plotted in dimensionless form because they depend on estimates of input resistance, which are difficult to make in cells with a prominent voltage-dependent current (I_h) that is active near resting potential. *D*: predicted magnitude spectra of responses (*top*) are significantly different in response to broadband (■) and theta-rich (●) inputs. Lower traces show the corresponding inputs. This prediction of significantly different response magnitude spectra in response to broadband and theta-rich stimuli is not seen in experimental data (*B*).

RMS value of fluctuating current input (σ_i) for inputs with different spectral contents. As one might expect, σ_v rises monotonically with σ_i in the subthreshold regime. Quantitatively, however, the results are incompatible with the hypothesis of subthreshold resonance. This point can be seen by comparing the measured family of curves in Fig. 5*A* with the "predicted" curves in Fig. 5*C*. (Predicted curves were constructed from responses to sinusoidal inputs, using the tenets of linear systems theory; see METHODS.) The predicted curves have notably different slopes, or gains, because the three types of input have different proportions of their power in the 4- to 12-Hz resonance band of the frequency response curve. A resonant cell should magnify those differences in input. Measured curves (Fig. 5*A*), on the other hand, have slopes that are very similar, and in fact statistically indistinguishable, as indicated by the interaction term from two-way ANOVA analysis ($P > 0.5$ in both cases for the null hypothesis regarding interaction; as before, nonoverlapping data sets were used to compare theta-rich responses with broadband and sub-theta responses). These results indicate that SCs are nonresonant for noise-like stimuli or at least far less resonant than predicted by responses to sinusoidal stimuli. Instead, the SC output was remarkably similar in total level of fluctuation, regardless of the frequency content of the stimulus.

To investigate the notion of subthreshold resonance in more detail, we compared the frequency profiles of recorded subthreshold responses to broadband and theta-rich inputs (Fig. 5*B*) with the profiles predicted by sinusoidal inputs and linear systems analysis (Fig. 5*D*; see METHODS). Output spectra (Fig. 5*B*, *top*) are elevated in the theta band compared with input spectra (Fig. 5*B*, *bottom*). However, the more striking effect lies in comparing responses produced by broadband and theta-rich stimulation. Spectra of recorded responses (Fig. 5*B*, *top*) to these distinct stimuli are strikingly similar (although statistically distinct). Spectra of predicted responses (Fig. 5*D*, *top*; see METHODS) differ by a factor of 2–3 for lower frequencies, reflecting the differences in the two input types and the resonance predicted from sinusoidal responses. The diminishment of that difference in experimental data shows that SCs do not have a consistent input-output relationship, violating the fun-

damental property of additivity in linear systems. Together, the lack of correspondence between measured and predicted responses in Fig. 5 imply that SCs are both nonresonant and nonlinear in response to noise-like stimuli.

DISCUSSION

SCs of the MEC relay information from the neocortex to the hippocampus. The striking temporal patterns seen in SCs with sub- and peri-threshold stimulation (Alonso and Klink 1993; Alonso and Llinás 1989), as well as the cells' inherent noisiness (White et al. 1998, 2000) suggest that SCs are likely to reshape and perhaps respond with selective reliability to the fluctuating inputs they receive in vivo. Our measurements of reliability in response to peri-threshold frozen noise inputs support the hypothesis that spiking SCs preferentially pass on inputs with significant power in the theta (4–12 Hz) frequency band. In contrast, subthreshold responses of SCs to frozen noise stimuli are not frequency-selective but seem to reflect the total power in the stimulus. We hypothesize that total power is "reported" in the magnitude of subthreshold oscillations. Together, these results indicate that SCs may be ideally driven by overall powerful stimuli (to initiate subthreshold oscillations) with episodes of appropriately phased theta-band stimuli (to induce spiking).

Frequency-sensitive reliability: relationship to previous studies

Frequency dependence of reliability has been noted in a number of experimental and theoretical studies, but in incompatible ways. For example, in recordings from neocortical pyramidal cells (Mainen and Sejnowski 1995; Nowak et al. 1997) and associated modeling and theoretical work (Cecchi et al. 2000; Schneidman et al. 1998), increased stimulus bandwidth gives increased reliability. This effect is often attributed to the fact that such stimuli have more fast transitions that drive spiking most effectively. Other experimental (Fellous et al. 2001; Hunter et al. 1998) and theoretical (Jensen 1998) studies suggest that the most effective stimulus contains the bulk of its power near the preferred spiking frequency of the cell for a given level of DC bias. Our results are compatible with this latter set, with the added twist that the unusual intrinsic dynamics of MEC SCs also shape their frequency-versus-current relationship and constrain the preferred spiking frequency to the theta band for a large range of input currents.

These conflicting forms of frequency dependence of reliability must relate either to subtle differences in experimental protocols or differences in cellular biophysical properties. In support of the latter possibility, effective stimuli with power near the mean spiking rate are often seen in cells with notably slow subthreshold dynamics that control spiking frequencies (Fellous et al. 2001; Hunter et al. 1998). However, our results indicate that the relationship between subthreshold dynamics and resonance in reliability is a subtle one and not as simple as it may seem.

Biophysical underpinnings of stimulus- and response-dependent resonance

Perhaps the most surprising, and revealing, result we report is that subthreshold resonance in SCs is conditional. For sinusoidal or ZAP stimuli, SCs show clear resonance of the form that one would predict from readily observed subthreshold oscillations (see review by Hutcheon and Yarom 2000). For more complex frozen noise stimuli, cursory examination of frequency response relationships to individual stimuli (Fig. 5*B*) indicates a similar result: relative to inputs, outputs have accentuated power in the 4- to 12-Hz band. However, comparison of results generated using multiple stimulus types at multiple RMS levels (Fig. 5, *A* and *B*) make it clear that SCs are remarkably insensitive to the distribution of frequencies within a subthreshold frozen noise stimuli. A practical consequence of our results is that one should interpret results of subthreshold resonance with caution: at least in MEC SCs, this property is fleeting and surprisingly stimulus-dependent. Our results indicate a biophysical mechanism of response to subthreshold stimulation that is notably nonlinear with the interesting tendency to "capture" total power in a complex input signal and shift that power into subthreshold oscillations at the theta frequency.

Given that the subthreshold responses to frozen noise stimuli show no sign of resonance, why is the resonance phenomenon so clear in reliability results in response to this class of stimulus? To us, this discrepancy indicates the existence of a resonating mechanism that is preferentially activated in the suprathreshold regime, akin to the medium afterhyperpolarization current described by Klink and Alonso (1997). The ionic mechanism underlying this suprathreshold resonance could be enhanced recruitment of the current that paces subthreshold oscillations (I_h and/or a slow K^+ current), or it could be molecularly distinct. In either case, this mechanism is driven more vigorously and coherently by spikes than by subthreshold activity and thus plays a larger role in selecting "effective," or temporally well-spaced, inputs in a band-pass manner. Taking this hypothesis further, we speculate that resonance is seen in spiking reliability and in subthreshold responses to sinusoids because, in both cases, there are features of each input (the spike events and evoked afterhyperpolarizations in 1 case, the regular stimulus peaks in the other) that serve as dependable "time marks," reliably resetting the cell's internal states closer to a given set of values with each occurrence of that feature and thus establishing the necessary conditions for a resonant response to stimuli with the appropriate frequency content.

We thank Drs. B. W. Connors, J. I. Luebke, and D. J. Pinto for invaluable technical assistance. We thank Drs. M. E. Hasselmo and D. J. Marr for beneficial comments and discussions, and A. D. Dorval for reading a previous version of this manuscript.

This work was supported by National Institute of Neurological Disorders and Stroke Grant (NS-34425) and National Science Foundation Grant (BES 0085177) to J. A. White.

REFERENCES

ALONSO A AND KLINK R. Differential electroresponsiveness of stellate and pyramidal-like cells of medial entorhinal cortex layer II. *J Neurophysiol* 70: 128–143, 1993.

ALONSO A AND LLINÁS RR. Subthreshold Na^+-dependent theta-like rhythmicity in stellate cells of entorhinal cortex layer II. *Nature* 342: 175–177, 1989.

BLAND BH AND COLOM LV. Extrinsic and intrinsic properties underlying oscillation and synchrony in limbic cortex. *Prog Neurobiol* 41: 157–208, 1993.

CECCHI GA, SIGMAN M, ALONSO JM, MARTINEZ L, CHIALVO DR, AND MAGNASCO MO. Noise in neurons is message dependent. *Proc Natl Acad Sci USA* 97: 5557–5561, 2000.

DESTEXHE A AND PARE D. Impact of network activity on the integrative properties of neocortical pyramidal neurons in vivo. *J Neurophysiol* 81: 1531–1547, 1999.

DICKSON CT, MAGISTRETTI J, SHALINSKY MH, FRANSEN E, HASSELMO ME, AND ALONSO A. Properties and role of I_h in the pacing of subthreshold oscillations in entorhinal cortex layer II neurons. *J Neurophysiol* 83: 2562–2579, 2000.

EDER C, FICKER E, GÜNDEL J, AND HEINEMANN U. Outward currents in rat entorhinal cortex stellate cells studied with conventional and perforated patch recordings. *Eur J Neurosci* 3: 1271–1280, 1991.

FELLOUS J-M, HOUWELING AR, MODI RH, RAO RPN, TIESINGA PHE, AND SEJNOWSKI TJ. The frequency dependence of spike timing reliability in cortical pyramidal cells and interneurons. *J Neurophysiol* 85: 1782–1787, 2001.

GUTFREUND Y, YAROM Y, AND SEGEV I. Subthreshold oscillations and resonant frequency in guinea pig cortical neurons: physiology and modelling. *J Physiol (Lond)* 483: 621–640, 1995.

HAAS JS AND WHITE JA. Reliability in neurons with intrinsically noisy oscillatory dynamics. *Bull Am Phys Soc* 44: 1228, 1999.

HAAS JS AND WHITE JA. Nonlinear resonance in oscillatory neurons of the medial entorhinal cortex. *Soc Neurosci Abstr* 26: 1264, 2000.

HASSELMO ME, FRANSEN E, DICKSON C, AND ALONSO AA. Computational modeling of entorhinal cortex. *Ann NY Acad Sci* 911: 418–446, 2000.

HUNTER JD, MILTON JG, THOMAS PJ, AND COWAN JD. Resonance effect for neural spike time reliability. *J Neurophysiol* 80: 1427–1438, 1998.

HUTCHEON B, MIURA RM, AND PUIL E. Subthreshold membrane resonance in neocortical neurons. *J Neurophysiol* 76: 683–697, 1996.

HUTCHEON B AND YAROM Y. Resonance, oscillation and the intrinsic frequency preferences of neurons. *Trends Neurosci* 23: 216–222, 2000.

JENSEN RV. Synchronization of randomly driven nonlinear oscillators. *Phys Rev E* 58: R6907–R6910, 1998.

KLINK R AND ALONSO A. Ionic mechanisms for the subthreshold oscillations and differential electroresponsiveness of medial entorhinal cortex layer II neurons. *J Neurophysiol* 70: 144–157, 1993.

KLINK R AND ALONSO A. Muscarinic modulation of the oscillatory and repetitive firing properties of entorhinal cortex layer II neurons. *J Neurophysiol* 77: 1813–1828, 1997.

MAINEN ZF AND SEJNOWSKI TJ. Reliability of spike timing in neocortical neurons. *Science* 268: 1503–1506, 1995.

NOWAK LG, SANCHEZ-VIVES MV, AND MCCORMICK DA. Influence of low and high frequency inputs on spike timing in visual cortical neurons. *Cereb Cortex* 7: 487–501, 1997.

PUIL E, GIMBARZEVSKY B, AND MIURA RM. Quantification of membrane properties of trigeminal root ganglion neurons in guinea pigs. *J Neurophysiol* 55: 995–1016, 1986.

SCHNEIDMAN E, FREEDMAN B, AND SEGEV I. Ion channel stochasticity may be critical in determining the reliability and precision of spike timing. *Neural Comput* 10: 1679–1703, 1998.

WHITE JA, BUDDE T, AND KAY AR. A bifurcation analysis of neuronal subthreshold oscillations. *Biophys J* 69: 1203–1217, 1995.

WHITE JA, KLINK R, ALONSO A, AND KAY AR. Noise from voltage-gated ion channels may influence neuronal dynamics in the entorhinal cortex. *J Neurophysiol* 80: 262–269, 1998.

WHITE JA, RUBINSTEIN JT, AND KAY AR. Channel noise in neurons. *Trends Neurosci* 23: 131–137, 2000.

WITTER MP, GROENEWEGEN HJ, LOPES DA SILVA FH, AND LOHMAN AH. Functional organization of the extrinsic and intrinsic circuitry of the parahippocampal region. *Prog Neurobiol* 33: 161–253, 1989.